A CA-CFAR AND LOCALIZED WAVELET SHIP DETECTOR FOR SENTINEL-1 IMAGERY

[†‡]C.P. Schwegmann,[†‡]W. Kleynhans,[⋆‡]B.P. Salmon and [†‡]L. Mdakane

[†]Department of Electrical, Electronic and Computer Engineering, University of Pretoria, South Africa

[‡]Remote Sensing Research Unit, Meraka Institute, CSIR, Pretoria, South Africa
cschwegmann@csir.co.za

[⋆]School of Engineering, University of Tasmania, Australia

ABSTRACT

The Maritime Domain Awareness initiative seeks to constantly improve the ways in which maritime information is collected. With the recent release of free Sentinel-1 imagery to the public, monitoring the maritime environment has become a more affordable. Using the basis of a cell-averaging constant false alarm rate prescreening method as input, this paper presents a novel method for detecting ships within Synthetic Aperture Radar imagery using a Gabor wavelet correlator. The method proposed allows for any configuration of the filter bank and prevents false detections by processing possible targets at a local scale. The method was tested against two Sentinel-1 images in both HH and HV polarization with a total of 82 ships. The method provided significantly improved FAR over the conventional CA-CFAR method at the cost of slightly worse detection accuracies in some cases.

***Index Terms*—** Marine technology, Synthetic aperture radar (SAR), Image Processing, Wavelet transforms

1. INTRODUCTION

One of the primary facets of Maritime Domain Awareness (MDA) is the policing and monitoring of ocean areas [1, 2]. It is prohibitively expensive to manually monitor coastlines and further out to sea so alternative methods of monitoring areas of the ocean is required. One such monitoring method, Synthetic Aperture Radar imagery, allows for a large portion of a country's ocean area to be viewed in a single image. With the advent of freely available data such as that of the Sentinel-1 mission (see Fig. 1), the cost of monitoring is further reduced. Ships have conventionally been monitored with onboard transponders but these run the risk of being sabotaged. As such advanced methods of ship detection using SAR have been developed to help improve the conventional method of ship monitoring. Advances to ship detection within SAR imagery have primarily focused on using the input images in the spatial domain [1, 3]. An alternative manner in which SAR images have been processed to detect ships is by applying a wavelet correlator to the input image to process the image in the spatial and frequency domain [4, 5]. The method presented in this paper uses a localized approach to ship detection by combining a conventional ship prescreening method with the advantages of a more advanced wavelet correlation scheme.

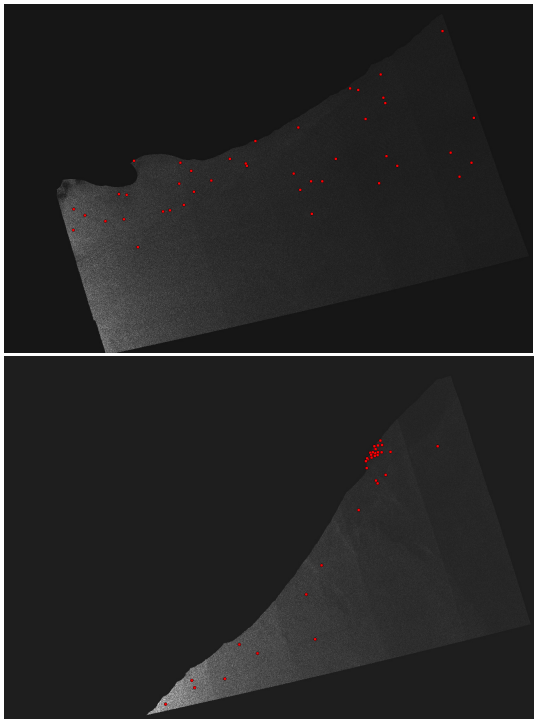

Fig. 1. Overview of the two Sentinel-1 EW SAR HH-polarized images, taken on the 6 and 8 October 2014 respectively. All land was removed from the input and the ships identified within the image are shown as red dots.

2. DATA DESCRIPTION

Two Extra Wide Swath Mode (EW) Sentinel-1 Synthetic Aperture Radar (SAR) images were used in this study. Each image has a spatial resolution of $20\,\text{m} \times 40\,\text{m}$ with a swath width of $400\,\text{km}$ in two polarizations namely HH and HV. The images were taken on 2014/10/06 and 2014/10/08 respectively. The images were acquired on the South African coast covering the cities of Port Elizabeth and Durban with a total of 82 ships. Two HH polarization images with all the land removed are shown in Fig. 1.

3. METHODOLOGY

The proposed method uses a series of steps to perform ship detection. A low-threshold cell-averaging constant false alarm rate (CA-CFAR) prescreening method is first applied to the SAR imagery. This locates the most likely regions of the SAR image to contain ships or areas with bright local intensity changes. Following this, each detected position is fed as a sub-image into the localized Gabor wavelet correlator. Unlike previous wavelet correlators [4, 5], the proposed correlator applies no restrictions to the number of wavelet filter banks applied to the image. Furthermore, by concentrating on sub-images of possible targets the number of false alarms is reduced compared to processing the entire SAR image at once. The various Gabor wavelet filtered sub-images are all spatially correlated together to generate a sub-image indicating the pixels with the highest correlation. This sub-image is then thresholded to obtain a binary image that indicates if the current position contains a ship or not. The following sections provides more details for these methods.

3.1. CA-CFAR prescreening

The purpose of a CFAR prescreening method is use a given threshold or FAR across the entire image to select targets that are abnormally bright compared to their neighbors in a local sense. Typically, a single threshold is selected and the local statistics of the region of interest (ROI) and its background are computed and compared against the given threshold to determine if the ROI is a bright area or not. The CA-CFAR prescreening method uses the mean pixel values for the clutter and ROI windows for the image statistics [6, 7, 8, 3, 9, 10]. In some versions of the CFAR (and CA-CFAR) prescreening method a different threshold is assigned to each pixel and used in conjunction with the ROI's statistics to determine if a pixel is bright or not [2]. For the purpose of this study a single, low-valued threshold CA-CFAR detector is used to highlight possible ships with a window configuration shown in Fig. 2.

Assuming an input Sentinel-1 SAR intensity image $\mathbf{I}$ with image dimensions $X \times Y$ where $x = \{0, \ldots, X-1\}$, $y = \{0, \ldots, Y-1\}$ and $x, y \in \mathbb{N}$ and such that image $\mathbf{I}$ can be defined as.

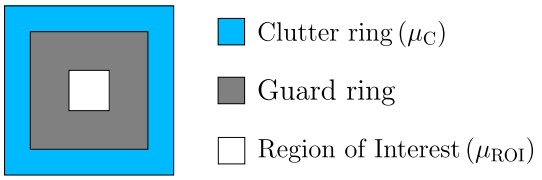

Fig. 2. CA-CFAR Neighborhood scheme used for this study. The values μ_C and μ_{ROI} represent the mean clutter and Region of Interest (ROI) pixel values. The clutter ring is used to calculate each ROI's mean ocean backscatter whereas the clutter mean is in place to prevent corruption of the clutter mean by the brighter objects larger than the ROI.

$$\mathbf{I} = \left\{ \left\{ I(x,y) \right\}_{x=0}^{x=X-1} \right\}_{y=0}^{y=Y-1} \tag{1}$$

$$= \begin{bmatrix} I(0,0) & \cdots & I(0,Y-1) \\ I(1,0) & \cdots & I(1,Y-1) \\ \vdots & \ddots & \vdots \\ I(X-1,0) & \cdots & I(X-1,Y-1) \end{bmatrix}. \tag{2}$$

The CA-CFAR prescreening method produces a binary output image $\mathbf{J}(\mathbf{I}, T)$ from the input image defined in (2) using

$$\mathbf{J}(\mathbf{I}, T) = \left\{ \left\{ J(\mathbf{I}, x, y, T) \right\}_{x=0}^{x=X-1} \right\}_{y=0}^{y=Y-1}. \tag{3}$$

where T is known as the CA-CFAR threshold and is inversely proportional to the number of false alarms permissible. The CA-CFAR binary image $J(\mathbf{I}, x, y, T)$ is calculated with

$$J(\mathbf{I}, x, y, T) = \begin{cases} \text{true} & \text{if } \mu_{\text{ratio}}(x,y) > T \\ \text{false} & \text{otherwise} \end{cases}. \tag{4}$$

The quantity $\mu_{\text{ratio}}(x,y)$ is known as the mean (power) ratio and is defined as

$$\mu_{\text{ratio}}(x,y) = \frac{\mu_{\text{ROI}}(x,y)}{\mu_C(x,y)}, \tag{5}$$

$\mu_{\text{ROI}}(x,y)$ and $\mu_C(x,y)$ are known as the mean region of interest and mean clutter respectively and are calculated using the window system shown in Fig. 2.

3.2. Gabor Wavelet Correlation

Once all the possible candidate ships have been highlighted using the CA-CFAR prescreening method then a sub-image around each possible detection is extracted. The sub-image $\mathbf{S}$ with image dimensions $N \times M$ where $n = \{0, \ldots, N-1\}$, $m = \{0, \ldots, N-1\}$ and $m, n \in \mathbb{N}$ is processed using the Gabor wavelet correlator. The size of the sub-image depends on the maximum size of the ship and for this study it was

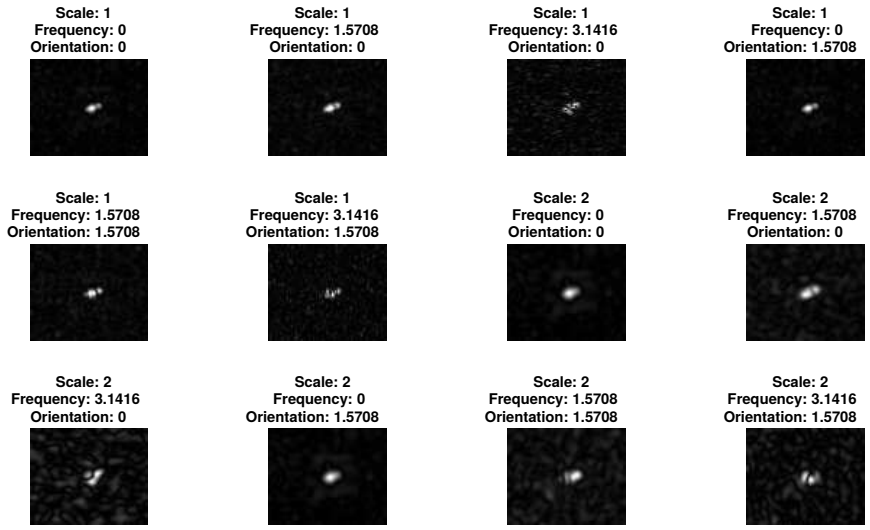

Fig. 3. Sentinel-1 sub-image $\mathbf{S}$ (top-left) processed at two scales, two orientations and two frequencies. All 12 of these images are multiplied together to obtain $\mathbf{W}$ for this sub-image.

assumed that any single ship would fit within $M = N = 100$. The sub-image $\mathbf{S}$ is processed at various scales α_i where $i = 1 \dots a$, rotations ω_j where $j = 1 \dots b$ and frequencies ν_k where $k = 1 \dots c$. This generates $a \cdot b \cdot c$ sub-images. So for each scale, rotation and frequency, a Gabor filtered sub-image $\mathbf{G}_{\alpha_i,\omega_j,\nu_k}$ is generated from $\mathbf{S}$ using the function $G(\mathbf{S}, \alpha_i, \omega_j, \nu_k,)$. All $\mathbf{G}$ are multiplied together to generate the final sub-image $\mathbf{W}$ such that

$$\mathbf{W} = \prod_{i=1}^{a} \prod_{j=1}^{b} \prod_{k=1}^{c} \mathbf{G}_{\alpha_i,\omega_j,\nu_k} \tag{6}$$

$$\mathbf{G}_{\alpha_i,\omega_j,\nu_k} = \left\{ \left\{ G(\mathbf{S}, \alpha_i, \omega_j, \nu_k,) \right\}_{n=0}^{n=N-1} \right\}_{m=0}^{m=M-1}. \tag{7}$$

Fig. 3 show the results of processing a single sub-image $\mathbf{S}$ at two scales, two orientations and three frequencies. All of these are correlated together to generate $\mathbf{W}$ which is then thresholded to detect whether it contains a ship or not.

3.3. Sub-image thresholding

The final step of the method is to threshold the sub-image $\mathbf{W}$ using a threshold value of T_{si}. The value T_{si} determines the minimum level of correlation between sub-imagesl. If any pixels in $\mathbf{W}$ are above T_{si} then the image contains a ship. Fig. 3 show an example of the various Gabor filtered images G for a sub-image S containing a ship. Each sub-image $\mathbf{W}$ is classified as having a ship or not using

$$\text{Ship Detected} = \begin{cases} \text{true}, & \text{if any } \mathbf{W} > T_{\text{si}} \\ \text{false}, & \text{otherwise} \end{cases}. \tag{8}$$

3.4. Benefits of proposed method

This prescreening method provides a number of benefits above other methods. Parallel sub-image generation, correlation and rapid thresholding means very little overhead is caused above that of a CA-CFAR prescreening method. The proposed method imposes no limit on the configuration of the Gabor wavelet filter bank, unlike previous methods [4, 5]. This also means that a specific filtering set can be created - for instance, only filtering the sub-images using specific orientations and keeping the scales and frequencies fixed.

By processing sub-images of possible targets rather than the whole SAR image, higher backscatter areas within the SAR image (near the nadir) are analyzed at a local scale. This prevents their relative brightness from causing false detections unlike when using a global thresholding method [4]. Finally, no training data is used for this prescreening method so the method can be extended to newer datasets without extensive retraining of a classifier [1].

4. RESULTS

The proposed ship detection method was compared using two metrics, Detection Accuracy and False Alarm Rate (FAR). Detection Accuracy is a measure of the number of correct detections or true positives obtained by the method whereas FAR is the number of false alarms divided by the total number of pixels tested for that image. The proposed method was tested against a CA-CFAR method to determine if the method is a viable ship detection method. The performance for the proposed CA-CFAR Gabor wavelet prescreening method is shown in Table 1. The method is compared to a conventional CA-CFAR with a region of interest window size of 1×1, a

Table 1. Detection Accuracy and False Alarm Rate (in parenthesis) for the two images with the conventional CA-CFAR and CA-CFAR Gabor Wavelet Correlator methods.

Method	Image 1 (HH)	Image 1 (HV)	Image 2 (HH)	Image 2 (HV)
CA-CFAR	$97.61\%\ (1.85 \times 10^{-5})$	$95.91\%\ (8.93 \times 10^{-6})$	$96.96\%\ (1.98 \times 10^{-6})$	$100.0\%\ (1.33 \times 10^{-6})$
Gabor CA-CFAR	$92.86\%\ (2.49 \times 10^{-6})$	$91.83\%\ (1.89 \times 10^{-6})$	$90.91\%\ (3.84 \times 10^{-6})$	$96.97\%\ (3.25 \times 10^{-6})$

guard window size of 11×11, background window size of 21×21 and threshold value of $T = 3.5$. The CA-CFAR correlator used the same CA-CFAR parameters except for the threshold value which was set to $T = 2.5$. The proposed method parameters were: $\alpha = \{1, 2\}, \omega = \{0, \frac{\pi}{2}\}, \nu = \{0, \frac{\pi}{2}, \pi\}$, $T_{\text{si}} = 0.5$ and $M = N = 100$.

The results are presented first with the Detection Accuracy (DA) followed by the False Alarm Rate (FAR) in parenthesis. The proposed method had considerably better FAR for both polarizations of Image 1 and slightly lower detection accuracies than the standard CA-CFAR method. Conversely, the results for the second image was slightly better for the conventional CA-CFAR method than the proposed method. This could be due to incorrect parameter selection as both images were processed using the same parameters which may not be ideal.

5. CONCLUSION

In this paper a novel method that combines the CA-CFAR prescreening method with a Gabor wavelet based correlator is used to detect ships in SAR imagery. The method exploits the fact that noise (sea backscatter) decorrelates across multiple wavelet images whilst objects like ships will appear to have a strong signal at different frequencies, orientations and scales. The method approaches the problem from a local perspective by first applying a CA-CFAR and then processes each possible detection sub-image using the Gabor wavelet correlator. The method was tested against Sentinel-1 data and initial results indicate a similar level of performance to that of the standard CA-CFAR detector with the possibility of much improved performance in some cases. Initial results indicate reasonable performance within the new Sentinel-1 data and further adjustments to the method should lead to an improved ship detection method when compared to previous wavelet-based ship detection methods.

6. REFERENCES

[1] C. P. Schwegmann, W. Kleynhans, and B. P. Salmon, "Ship Detection in South African oceans using SAR, CFAR and a Haar-like Feature Classifier," in *Geoscience and Remote Sensing Symposium, 2014. IGARSS 2014. IEEE International*, 2014, pp. 557–560.

[2] C. Schwegmann, W. Kleynhans, and B. Salmon, "Manifold Adaptation for Constant False Alarm Rate Ship Detection in South African Oceans," *IEEE Journal of Selected Topics in Applied Earth Observations and Remote Sensing*, vol. PP, no. 99, pp. 1–9, Apr. 2015.

[3] K. El-Darymli, P. McGuire, D. Power, and C. Moloney, "Target detection in synthetic aperture radar imagery: a state-of-the-art survey," *Journal of Applied Remote Sensinge*, vol. 7, no. 1, pp. 071598–071598, Mar. 2013.

[4] M. Tello, C. Lopez-Martinez, and J. J. Mallorqui, "A novel algorithm for Ship Detection in SAR imagery based on the Wavelet Transform," *IEEE Geoscience and Remote Sensing Letters*, vol. 2, no. 2, pp. 201–205, Apr. 2005.

[5] F. Berizzi D. Stagliano, A. Lupidi, "Ship detection from sar images based on CFAR and wavelet transform," in *2012 Tyrrhenian Workshop on Advances in Radar and Remote Sensing (TyWRRS)*, Sept. 2012, pp. 53–58.

[6] D. J. Crisp, "The State-of-the-Art in Ship Detection in Synthetic Aperture Radar Imagery," Tech. Rep. DSTO-RR-0272, Australian Department of Defence, Edinburgh, Australia, 2004.

[7] P. Lombardo, M. Sciotti, and L. M. Kaplan, "SAR prescreening using both target and shadow information," in *2001 IEEE Proc. Radar Conf.*, Atlanta, United States of America, May 2001, pp. 147–152.

[8] W. Kleynhans, B. P. Salmon, C. P. Schwegmann, and V. Seotlo, "Ship Detection in South African oceans using a combination of SAR and historic LRIT data," in *Geoscience and Remote Sensing Symposium, 2013. IGARSS 2013. IEEE International*, 2013, pp. 1–4.

[9] F. Bi, F. Pang, B. Zhu, and L. Chen, "A cascaded false-alarm elimination method for accurate ship detection in SAR images," in *Radar Conference 2013, IET International*, 2013, pp. 1–4.

[10] W. An, C. Xie, and X. Yuan, "An Improved Iterative Censoring Scheme for CFAR Ship Detection With SAR Imagery," *IEEE Transactions on Geoscience and Remote Sensing*, vol. 52, no. 8, pp. 4585–4595, Aug. 2014.